



## The 270 MeV deuteron beam polarimeter at the Nuclotron Internal Target Station

P.K. Kurilkin<sup>a,k</sup>, V.P. Ladygin<sup>a,k,\*</sup>, T. Uesaka<sup>b</sup>, K. Suda<sup>c</sup>, Yu.V. Gurchin<sup>a</sup>, A.Yu. Isupov<sup>a</sup>, K. Itoh<sup>d</sup>, M. Janek<sup>a,e</sup>, J.-T. Karachuk<sup>a,f</sup>, T. Kawabata<sup>b</sup>, A.N. Khrenov<sup>a</sup>, A.S. Kiselev<sup>a</sup>, V.A. Kizka<sup>a</sup>, J. Kliman<sup>g</sup>, V.A. Krasnov<sup>a,h</sup>, A.N. Livanov<sup>a,h</sup>, Y. Maeda<sup>i</sup>, A.I. Malakhov<sup>a</sup>, V. Matousek<sup>g</sup>, M. Morhach<sup>g</sup>, S.G. Reznikov<sup>a</sup>, S. Sakaguchi<sup>b</sup>, H. Sakai<sup>b,j</sup>, Y. Sasamoto<sup>b</sup>, K. Sekiguchi<sup>c</sup>, I. Turzo<sup>g</sup>, T.A. Vasiliev<sup>a,k</sup>

<sup>a</sup> Joint Institute for Nuclear Research, Dubna, Russia

<sup>b</sup> Center for Nuclear Study, University of Tokyo, Tokyo 113-0033, Japan

<sup>c</sup> RIKEN Nishina Center, Saitama, Japan

<sup>d</sup> Department of Physics, Saitama University, Saitama, Japan

<sup>e</sup> Physics Department, University of Žilina, 010 26 Žilina, Slovakia

<sup>f</sup> Advanced Research Institute for Electrical Engineering, Bucharest, Romania

<sup>g</sup> Institute of Physics of Slovak Academy of Sciences, Bratislava, Slovakia

<sup>h</sup> Institute for Nuclear Research, Moscow, Russia

<sup>i</sup> Kyushu University, Hakozaki, Japan

<sup>j</sup> University of Tokyo, Tokyo, Japan

<sup>k</sup> Moscow State Institute of Radio-engineering Electronics and Automation (Technical University), Moscow, Russia

### ARTICLE INFO

#### Article history:

Received 4 May 2010

Received in revised form

6 March 2011

Accepted 25 March 2011

Available online 2 April 2011

#### Keywords:

Deuteron–proton elastic scattering

Beam polarization

Analyzing powers

### ABSTRACT

A deuteron beam polarimeter has been constructed at the Internal Target Station at the Nuclotron of JINR. The polarimeter is based on spin-asymmetry measurements in the d–p elastic scattering at large angles and the deuteron kinetic energy of 270 MeV. It allows to measure vector and tensor components of the deuteron beam polarization simultaneously.

© 2011 Elsevier B.V. All rights reserved.

## 1. Introduction

One of the directions of nuclear spin physics at intermediate energies is the study of the spin structure of two- and three-nucleon forces in deuteron induced reactions. Such investigations with polarized deuterons have been performed recently at RARF [1–6], RCNP [7], KVI [8–13] and IUCF [14]. High accuracy polarization data have been obtained. Similar experiments have been proposed at the Nuclotron [15] and RIBF [16] to study the energy dependence of the spin structure of three-nucleon forces via measuring the deuteron analyzing powers in d–p elastic scattering.

However, these studies require the high precision polarimetry to obtain reliable values of beam polarization. Since deuteron is a spin-1 particle, the polarimetry should have the capability to determine simultaneously both vector and tensor components of

the beam polarization. Moreover, the effective analyzing powers of the polarimeter should be known with high precision to provide small systematic errors while determining the beam polarization components.

The d–p elastic scattering has been traditionally used for the tensor and vector polarimetry at intermediate and high energies. Earlier it had been demonstrated that d–p elastic scattering at forward angles had large vector  $A_y$  and tensor  $A_{yy}$  analyzing powers at 1600 MeV [17] and could be used for polarization analysis [18,19]. The measurements at forward angles require sophisticated equipment to identify the events. For example, in Ref. [17], deuterons scattered at  $\theta_{lab}^d = 7.5^\circ$  from a hydrogen target were selected by the two-arm magnetic spectrometer ALPHA from the deuterons of other reaction channels and other particles. The same method has been applied recently at COSY using the ANKE spectrometer [20] at the initial deuteron energy of 1170 MeV and  $4^\circ \leq \theta_{lab}^d \leq 10^\circ$  where the vector and tensor analyzing powers are large [18,21].

The d–p elastic scattering at large angles ( $\theta_{cm} \geq 60^\circ$ ) has been successfully used for the deuteron polarimetry at RIKEN at a few

\* Corresponding author at: Joint Institute for Nuclear Research, Dubna, Russia.  
E-mail address: [vladygin@jinr.ru](mailto:vladygin@jinr.ru) (V.P. Ladygin).

hundreds of MeV. This reaction has several advantages as a beam-line polarimetry over the others. First, both the vector and tensor analyzing powers for the reaction have large values [1–3,22]. The values of the analyzing powers were obtained for the polarized deuteron beam, whose absolute polarization had been calibrated via the  $^{12}\text{C}(d,\alpha)^{10}\text{B}^*[2^+]$  reaction [4]. The accuracy of the determination of the deuteron beam polarization achieved with this method is better than 2%. Second, to identify the events, it is sufficient to carry out kinematical coincidence measurements of deuteron and proton by means of simple plastic scintillation counters. It is justified because the backgrounds event rate is smaller for kinematics chosen than for the small scattering angles in c.m.

The d–p elastic scattering at  $\theta_{\text{cm}} = 101.2^\circ$  has been also used to determine the beam polarization at 130 MeV at KVI [23]. Later for the deuteron polarimetry at KVI the values of the analyzing powers of the d–p elastic scattering at large angles in c.m. at 130 and 180 MeV were determined in a dedicated experiment performed at RIKEN [6], using absolute calibration of the beam polarization via the  $^{12}\text{C}(d,\alpha)^{10}\text{B}^*[2^+]$  reaction [4]. The d–p elastic scattering at 270 MeV and large scattering angles has been used recently to measure the vector and tensor deuteron beam polarization at COSY [20] with the EDDA polarimeter [24].

The goal of the present article is to report about a new polarimeter based on the asymmetry measurements in d–p elastic scattering at 270 MeV at the Internal Target Station (ITS) [25] of the Nuclotron (LHEP-JINR). The paper is organized as follows. The details of the polarimeter construction are given in Section 2. The experimental and data analysis procedures are described in Section 3. The details of the beam polarization evaluation and results are given in Section 4. The conclusions are drawn in the last Section.

## 2. Polarimeter

Efficient polarimetry can be provided even for rather low beam intensity using a thin solid internal target inside the accelerator ring. Due to multi-passage of the beam through the target point, the luminosity can be significantly increased by using a properly tuned internal target trajectory. Therefore, this internal beam polarimeter with a very thin target can have approximately the same performance as external beam polarimeters.

The deuteron beam polarimeter was installed at the ITS in the Nuclotron ring. The ITS consists of a spherical scattering chamber and a target sweeping system. The scattering chamber is fixed on the flanges of the Nuclotron ion tube. The disk with the slits where six different targets are mounted is located on the axle of the stepper motor. The selected target is turned to the center of the ion tube by the disk rotation when the particles are accelerated up to the required energy. A  $10\text{ }\mu\text{m}$   $\text{CH}_2$  film was used as a proton target for the polarimeter. The details of the ITS can be found in Ref. [25].

A schematic view of the polarimeter setup designed for the beam polarization measurements in a wide energy range [15] is shown in Fig. 1. A detector support with 46 mounted plastic scintillation counters is placed downstream the ITS spherical chamber. Each plastic scintillation counter was coupled to a photo-multiplier tube Hamamatsu H7416MOD. Nine proton detectors were installed for LEFT (LP1–9), as well as for RIGHT (RP1–9) and UP (UP1–9), but due to space limitation only four for DOWN (DP1–4). The proton detectors were placed at a distance of 600 mm from the target. The angular span of one proton detector was  $2^\circ$  in the laboratory frame, which corresponds to  $\sim 4^\circ$  in the c.m. system. Four deuteron detectors (LD1–4, RD1–4, DD1–4) were placed at scattering angles of deuterons coinciding kinematically with the protons. One deuteron detector (UD1) can cover the solid angle corresponding to DP1–4.

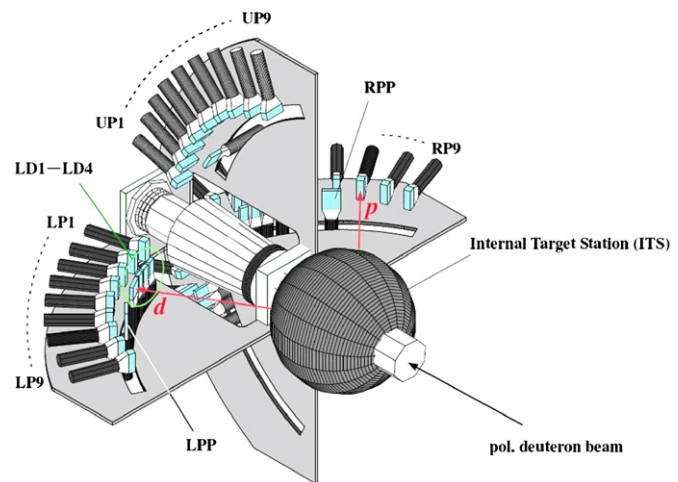


**Fig. 1.** A schematic view of the polarimeter setup installed downstream the ITS spherical chamber. Plastic scintillation counters coupled to PMTs are placed to the left, right, up, and down the beam axis.

**Table 1**

Plastic scintillation counters used for the polarimeter. The laboratory angles of the detectors at 270 MeV are shown in the last column.

	Width (mm)	Height (mm)	Thickness (mm)	LAB angle (deg)
Proton detectors	20	40/60	20	21.3, 26.1, 30.9, 35.8, 40.8, 45.0, 50.8, 55.9
Deuteron detectors	24	40	10	20.1, 22.7, 25.6
	50	40	10	29.3
Quasifree p–p detectors	50	60	10	44.0

In addition, one pair of detectors (LPP and RPP) was placed to register two protons from quasi-elastic p–p scattering at  $\theta_{pp} = 90^\circ$  in the c.m. in the horizontal plane. The deuteron and quasi-elastic p–p detectors were placed at a distance of 560 mm from the target in front of the proton detectors.

The scattered deuterons and recoil protons at 270 MeV were detected in kinematic coincidence over the c.m. angular range of  $65^\circ$ – $135^\circ$  at eight different angles, defined by the positions of the proton detectors LP1–8, RP1–8, UP1–8 and DP1–4. The angular range of the measurements (and number of angular setting) was defined by the behavior of the vector analyzing power  $A_y$  at 270 MeV, which has the values close to zero outside the c.m. angular range of  $65^\circ$ – $135^\circ$  [1,2,4]. Sizes of the detectors and their setting angles for 270 MeV are listed in Table 1.

For the internal beam polarimeter the luminosity depends both on the beam intensity and internal target trajectory. In this respect, a monitor reflecting the number of the beam-target interactions, has to be used to measure the luminosity. Additionally, the luminosity monitor for the polarization measurements has to be insensitive to the beam polarization. It uses quasi-elastic p–p scattering yield at  $\theta_{pp} = 90^\circ$  in the c.m. in the horizontal plane as it refers to these both luminosity monitor requirements. On the one hand, it is defined by the number of beam-target collisions. On the other hand, it is independent of the beam polarization value, because the analyzing power of p–p elastic scattering at  $\theta_{pp} = 90^\circ$  in the c.m. is equal to zero.

Anode signals from the photo-multiplier tubes were fed into the eight-channel constant-fraction discriminators (CFD), ORTEC CF8000, which has one analog output and three logic outputs for each

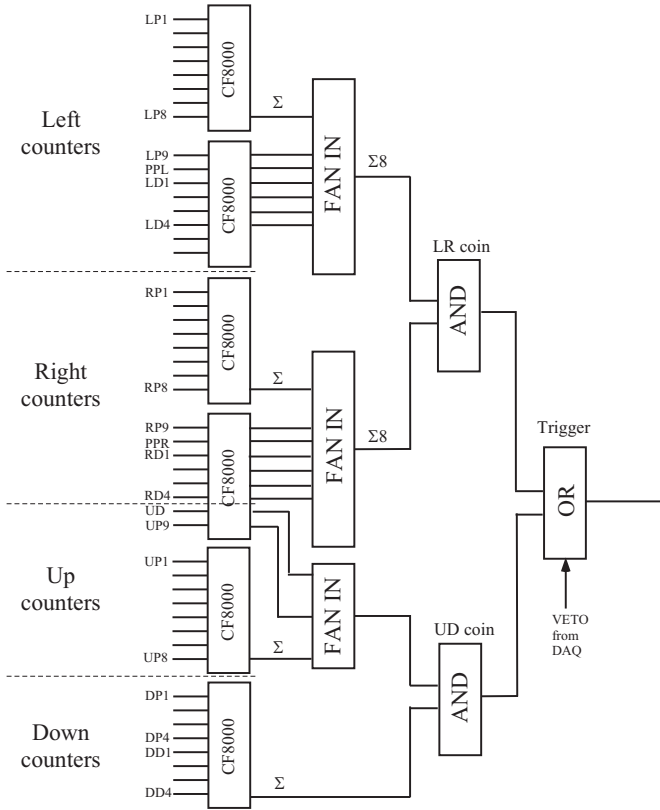


Fig. 2. Trigger logic for coincidences.

channel. The analog signals were transmitted to Fast-Encoding Read-out ADCs (FERA), LeCroy 4300B, through cable delays. One of the logic outputs was used to stop the Time-to-FERA Converter (TFC), LeCroy 4303. The other two logic outputs made a logical AND which corresponded to the coincidence between the scattered deuteron and the recoiling proton. As shown in Fig. 2, the coincidences of any of LEFT detectors (LP1–8, LD1–4, PPL) with any of the RIGHT detectors (RP1–8, RD1–4, PPR) are triggering the data taking. Coincidences between the UP and DOWN detectors were also used to make a trigger. The data were accumulated with a VME-CAMAC based data-acquisition system [26].

### 3. Experimental procedure

The polarized deuteron beam was provided by the atomic-beam polarized ion source POLARIS [27]. Nuclear polarization is provided via radio-frequency (RF) hyperfine structure transitions. In this experiment the data were taken for three spin modes: unpolarized, “2–6” and “3–5”, which have theoretical maximum polarizations of  $(p_z, p_{zz}) = (0,0)$ ,  $(1/3,1)$  and  $(1/3,-1)$ , respectively. Two different RF cells of POLARIS [27] with the working frequencies of 384.9 and 320.1 MHz have been used to provide the “2–6” and “3–5” transitions, respectively. The spin modes were changed cyclically and spill-by-spill. The quantization axis was perpendicular to the beam-circulation plane of the Nuclotron.

The typical beam intensity in the Nuclotron ring was  $2-3 \times 10^7$  deuterons per spill with a duration of  $\sim 1$  s independently on the spin mode. The repetition rate and orbit frequency at 270 MeV were 1/6 Hz and 0.583 MHz, respectively. A 10  $\mu\text{m}$  CH<sub>2</sub> film was used as a proton target. No measurements with the carbon target were made, because the background from the carbon content of the CH<sub>2</sub> target measured at RIKEN was less than 1% at 270 MeV [1].

A signal from the target position monitor [28] was used to tune the accelerator parameters to bring the interaction point close to the center of the ITS chamber. The signals from the monitor were also stored as raw data so that one can use the position information in off-line analysis. The distribution of the interaction point in mm is shown in Fig. 3. The uncertainty of the interaction point is estimated to be of  $\pm 1$  mm. The details of the target position monitor operation are described in Ref. [28].

The d–p elastic events were selected by using the energy loss correlation and time-of-flight difference for the scattered deuteron and recoil proton.

Fig. 4 shows the energy loss correlation of proton and deuteron for the scattering angle of  $75^\circ$  in the c.m. One can see a prominent locus corresponding to the d–p elastic events. The solid line is a graphical cut for the selection of the d–p elastic events.

The final selection of the events used to deduce the spin-dependent asymmetry was made by the time difference between the signals for the conjugated deuteron and proton detectors. Fig. 5 shows the time difference between the signals for the deuteron and proton detectors at  $75^\circ$  in the c.m. The open histogram in the upper panel represents the time difference  $\Delta T_{RL}$  without the criteria on the signal amplitudes correlation. The grey histogram demonstrates the events corresponding to the area out of the graphic cut shown in Fig. 4 by the solid line. The time difference  $\Delta T_{RL}$  with the criteria on the signal amplitudes correlation is shown in the bottom panel in Fig. 5. The dashed lines in the bottom panel are the prompt timing windows to select d–p elastic events. The time difference spectra  $\Delta T_{RL}$  with the criteria on the signal amplitudes correlation have been fitted by the constant outside of the prompt timing windows for the background estimation. The remaining background within timing windows was found less than 1% for all the deuteron–proton detectors pairs. Note, the direct measurements of the carbon content have been performed in the test experiment with CH<sub>2</sub> and carbon targets at 270 MeV and at the scattering angle of  $86.5^\circ$  in the c.m. at Nuclotron [15]. The carbon background was found negligibly small being in agreement with RIKEN measurements [1].

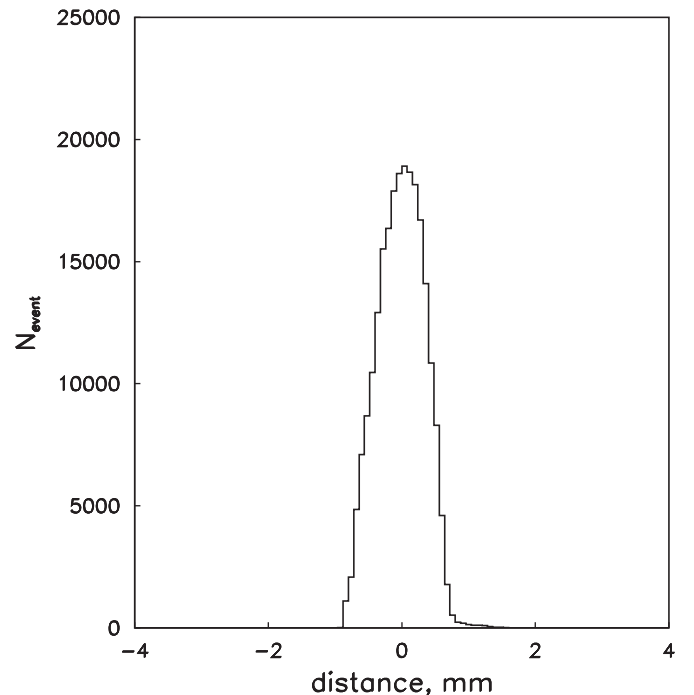


Fig. 3. Distribution of the interaction point in mm.

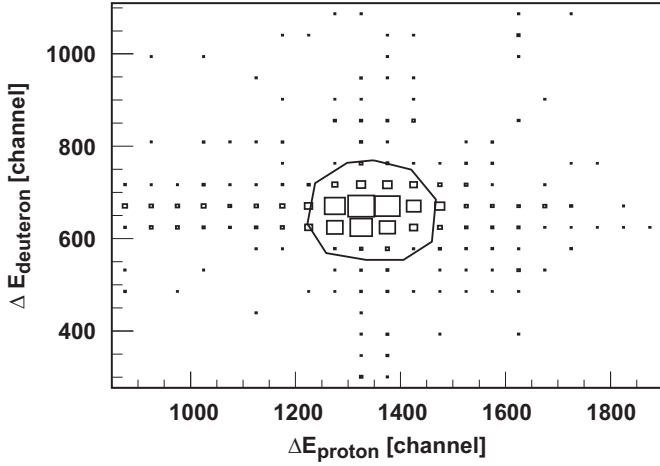


Fig. 4. The correlation of the amplitude signals for one pair of the deuteron and proton detectors at 270 MeV. The solid line is a graphical cut to select the d-p elastic events.

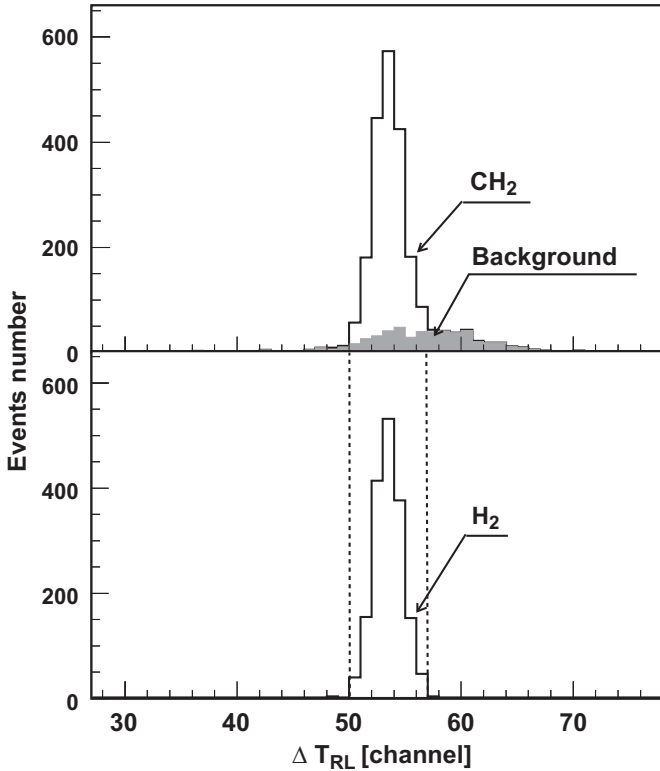


Fig. 5. The time difference between the signals for deuteron and proton detectors at 270 MeV and a scattering angle of 75° in the c.m.

#### 4. Deuteron beam polarization

The beam polarization was determined by using asymmetry of the d-p scattering yields and the known analyzing powers of the reaction [2,4]. Data at several scattering angles: 75°, 86.5°, 95°, 105°, 115°, 126.3° and 135°, were used to increase the polarimeter figure of merit. The values of the analyzing powers  $A_y$ ,  $A_{yy}$ ,  $A_{xx}$  and  $A_{xz}$  at these angles were obtained by the cubic spline interpolation of the data taken from Refs. [2,4]. The extrapolated values of the analyzing powers are shown in Fig. 6 with the solid circles and given in Table 2. The open squares and triangles represent the data used for the extrapolation procedure from Refs. [2] and [3,4], respectively. The errors for the data from Refs. [2–4] were taken as quadrature root of the sum of squared statistical and systematic errors.

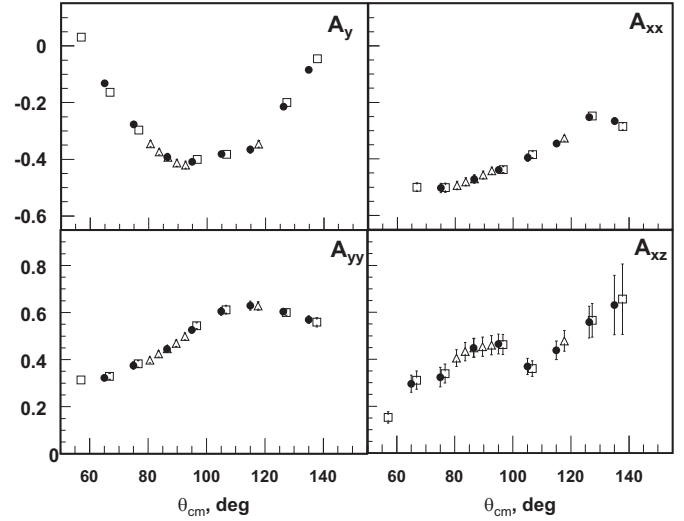


Fig. 6. Analyzing powers  $A_y$ ,  $A_{yy}$ ,  $A_{xx}$  and  $A_{xz}$  of d-p elastic scattering at 270 MeV as function of the scattering angle in the c.m. The open squares and triangles are the data from Refs. [2] and [3,4], respectively. The extrapolated values of the analyzing powers used to determine the deuteron beam polarization are shown with the solid circles.

Table 2

The extrapolated values of the analyzing powers  $A_y$ ,  $A_{yy}$ ,  $A_{xx}$  and  $A_{xz}$  for d-p elastic scattering at 270 MeV used to determine the deuteron beam polarization values.

$\theta_{c.m.}$ (deg)	$A_y$	$dA_y$	$A_{yy}$	$dA_{yy}$	$A_{xx}$	$dA_{xx}$	$A_{xz}$	$dA_{xz}$
65	-0.133	0.004	0.323	0.012	–	–	0.296	0.037
75	-0.277	0.004	0.375	0.016	-0.503	0.016	0.324	0.042
86.5	-0.392	0.012	0.445	0.013	-0.471	0.014	0.445	0.040
95	-0.410	0.009	0.526	0.014	-0.439	0.012	0.465	0.042
105	-0.382	0.004	0.605	0.017	-0.395	0.013	0.370	0.034
115	-0.367	0.012	0.629	0.019	-0.345	0.011	0.439	0.039
126.3	-0.216	0.007	0.604	0.011	-0.253	0.008	0.558	0.067
135	-0.084	0.005	0.570	0.016	-0.266	0.012	0.631	0.126

The d-p scattering yields in “2–6” and “3–5” spin modes are normalized on the yield for the unpolarized mode after correction of the integrated beam intensity and dead time of the data-taking system. For this purpose the absolute value of beam intensity is not necessary and the relative value monitored by the quasi-elastic p-p scattering is sufficient.

The normalized yields of the d-p elastic events for the left (L), right (R), up (U) and down (D) scattering:

$$L = 1 + \frac{2}{3} p_y A_y + \frac{1}{3} (2p_{xx} + p_{yy}) A_{xx} + \frac{1}{3} (2p_{yy} + p_{xx}) A_{yy} \quad (1)$$

$$R = 1 - \frac{2}{3} p_y A_y + \frac{1}{3} (2p_{xx} + p_{yy}) A_{xx} + \frac{1}{3} (2p_{yy} + p_{xx}) A_{yy} \quad (2)$$

$$U = 1 + \frac{1}{3} (2p_{yy} + p_{xx}) A_{xx} + \frac{1}{3} (2p_{xx} + p_{yy}) A_{yy} \quad (3)$$

$$D = 1 + \frac{1}{3} (2p_{yy} + p_{xx}) A_{xx} + \frac{1}{3} (2p_{xx} + p_{yy}) A_{yy} \quad (4)$$

were used to determine the beam polarization. Here,  $A_y$ ,  $A_{yy}$  and  $A_{xx}$  denote the deuteron analyzing powers,  $p_y$ ,  $p_{yy}$  and  $p_{xx}$  are the corresponding components of the beam polarization expressed as

$$p_y = p_z \sin \beta \cos \phi \quad (5)$$

$$p_{xx} = \frac{1}{2} p_z (3 \sin^2 \beta \sin^2 \phi - 1) \quad (6)$$

$$p_{yy} = \frac{1}{2} p_z (3 \sin^2 \beta \cos^2 \phi - 1), \quad (7)$$

where  $p_z$  and  $p_{zz}$  are the vector and tensor polarizations of the beam, respectively,  $\beta$  and  $\phi$  are the angles defining the beam polarization direction [29].

The  $L$ ,  $R$ ,  $U$  and  $D$  yields of d–p elastic scattering events at the scattering angles  $\theta_{cm} \geq 105^\circ$  were used; while only the  $L$ ,  $R$  and  $D$  yields at the angles of  $75^\circ$ ,  $86.5^\circ$  and  $95^\circ$  were used to determine beam polarization values.

Fig. 7 displays the values of the tensor  $p_{yy}$  and vector  $p_y$  polarizations of the beam for “2–6” and “3–5” spin modes of POLARIS [27] as function of the deuteron scattering angle in the c.m. The error bars include both statistical and systematic errors which are related with the uncertainties in the values of the analyzing powers. One can see a good agreement of the polarization values obtained at different scattering angles in the c.m. The dashed lines in Fig. 7 represent the beam polarization values averaged over all the scattering angles.

The beam polarization was measured several times at 270 MeV during the experiment studying the analyzing powers in d–p elastic scattering at high energies [30]. Figs. 8 and 9 illustrate the polarization values for the spin modes “2–6” and “3–5” of POLARIS [27], respectively, as functions of the measurement time in hours. The horizontal error bars reflect the duration of the measurements. First measurement (at  $t \sim 85$  h) corresponds to the measurements performed during  $\sim 17$  h, while two other measurements (at  $t \sim 180$  and  $305$  h) were performed during  $\sim 6$  h. The beam intensity during the experiment decreased with the time. Estimated from p–p quasi-elastic scattering at  $90^\circ$  in c.m. the integrated luminosity was  $\mathcal{L} \sim 4.6 \times 10^{32}$ ,  $\sim 3.6 \times 10^{31}$  and  $\sim 3.1 \times 10^{31} \text{ cm}^{-2}$  for the measurements performed at  $\sim 85$ ,  $\sim 180$  and  $\sim 305$  h, respectively. As the result the error bars for two last measurements of the beam polarization are much larger than for the first one.

Table 3 gives the values of the tensor  $p_{yy}$  and vector  $p_y$  polarizations of the beam for “2–6” and “3–5” spin modes of POLARIS [27] obtained for three separate measurements and averaged over the whole duration of the experiment. Both statistical and systematic errors due to the uncertainties in the values of the analyzing powers are shown in the above Table 3. These systematic errors do not exceed 1–2% for both the vector and tensor polarizations of the beam. One can see rather good time stability of the beam polarization values for the spin mode “2–6” during the experiment ( $\sim 220$  h) within the achieved accuracy of the measurements in contrast with the measurements

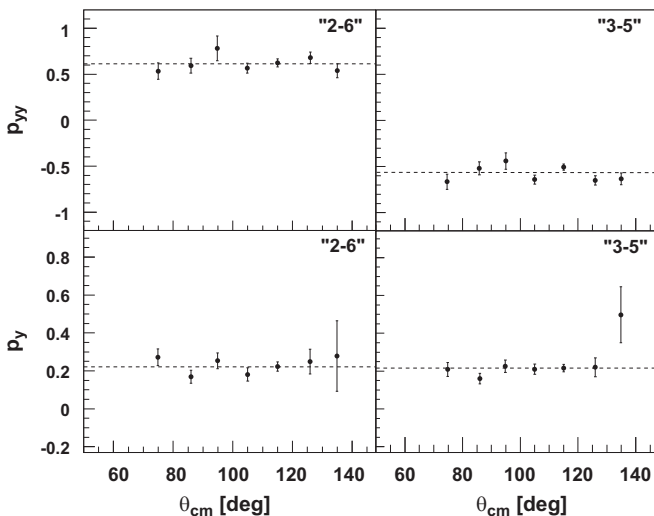


Fig. 7. Tensor  $p_{yy}$  and vector  $p_y$  polarizations of the beam for “2–6” and “3–5” spin modes of POLARIS [27] as function of the deuteron scattering angle in the c.m.

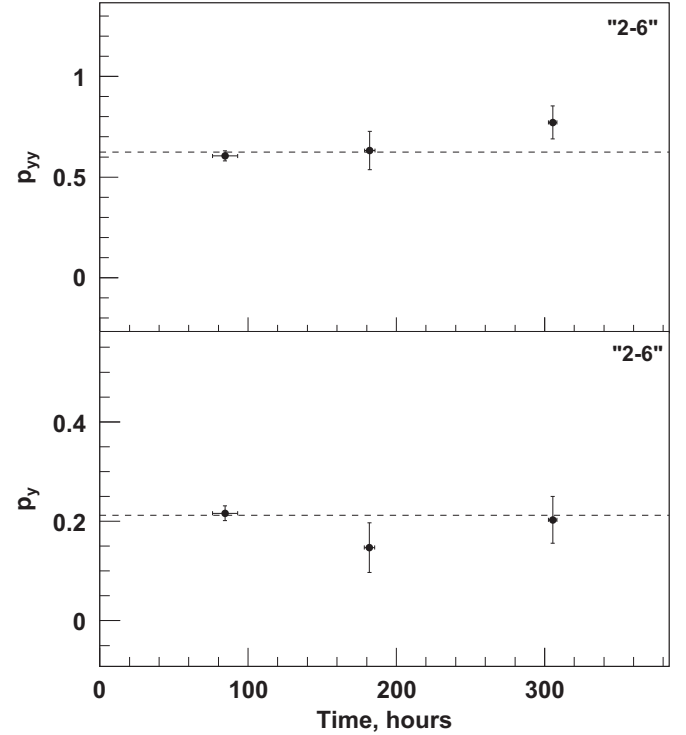


Fig. 8. Tensor  $p_{yy}$  and vector  $p_y$  polarizations of the beam for the spin mode “2–6” of POLARIS [27] versus the measuring time in hours.

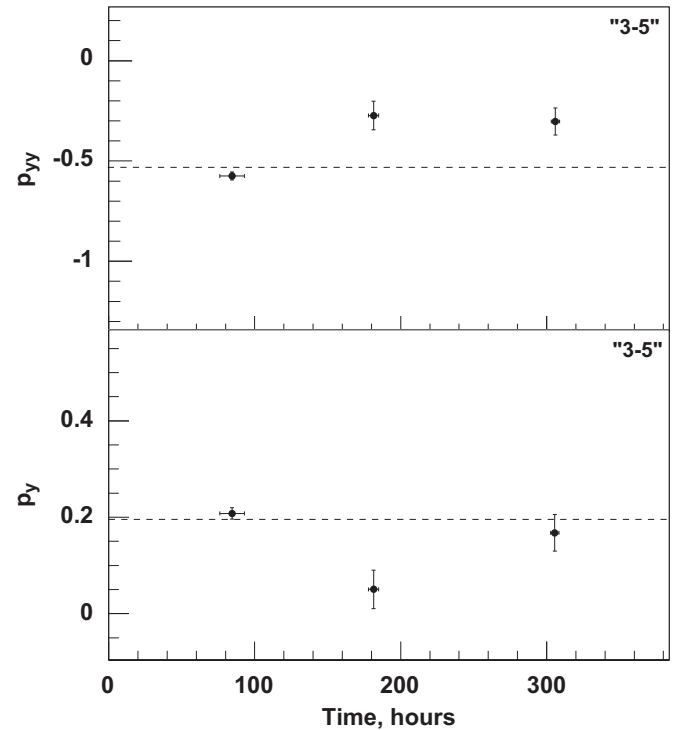


Fig. 9. Tensor  $p_{yy}$  and vector  $p_y$  polarizations of the beam for the spin mode “3–5” of POLARIS [27] versus the measurement time in hours.

for the spin mode “3–5”. The beam polarization values for the spin mode “3–5” for two last points deviate by  $3-4 \sigma$  from the averaged values of  $p_y$  and  $p_{yy}$ .

One of the reason of such deviation can be possible time dependence of the beam polarization for POLARIS [27]. The long-term stability of the deuteron beam polarization for POLARIS was



**Table 3**

The values of the vector  $p_y$  and tensor  $p_{yy}$  beam polarizations for the “2–6” and “3–5” spin modes of POLARIS [27].

Number of measurement	Spin mode	$p_y$	$\Delta p_y^{stat}$	$\Delta p_y^{sys}$	$p_{yy}$	$\Delta p_{yy}^{stat}$	$\Delta p_{yy}^{sys}$
1	“2–6”	0.216	0.014	0.002	0.605	0.024	0.005
	“3–5”	0.208	0.011	0.002	–0.575	0.020	0.005
2	“2–6”	0.146	0.050	0.004	0.632	0.094	0.011
	“3–5”	0.049	0.040	0.004	–0.281	0.071	0.007
3	“2–6”	0.201	0.047	0.003	0.767	0.082	0.009
	“3–5”	0.167	0.038	0.002	–0.303	0.067	0.003
Averaged	“2–6”	0.210	0.013	0.002	0.619	0.022	0.005
	“3–5”	0.193	0.011	0.002	–0.532	0.018	0.004

investigated in Refs. [17,31]. The good time stability for both vector and tensor components of the beam polarization was observed for the fixed working conditions of the ion source, the accelerator and beam transport system over 20 h of the accelerator [17]. However, possible time dependence of the beam polarization has been observed during 90 h [31]. If one assume the same linear decreasing of the asymmetries values with the time as in Ref. [31] one can expect the decreasing of the beam polarization values up to 30% for the whole duration of our experiment. However, the errors of the measurements for two last points in Figs. 8 and 9 are too large to draw the conclusion on the beam polarization time stability. Therefore, the systematic errors due to possible time dependence of the beam polarization values are not indicated in Table 3. The possible time dependence of the asymmetry values proofs the necessity of the beam polarization monitoring during the experiment.

The angle between the beam direction and polarization axis found from the Eqs. (1)–(4) and (5)–(7) was as  $\beta = -90.3 \pm 1.2^\circ$ , namely, the polarization axis was perpendicular to the plane containing the mean beam orbit in the accelerator.

The performance of the polarimeter is expressed in terms of the figure of merit,  $\mathcal{F}$ . It allows one to evaluate the counting rate  $N_{inc}$ , needed for the desired beam polarization accuracy  $\Delta P$ :

$$\Delta P \sim \frac{\sqrt{2}}{\mathcal{F} \sqrt{N_{inc}}} \quad (8)$$

$\mathcal{F}$  is a function of efficiency  $\varepsilon$  and analyzing power  $A$ . It is defined as

$$\mathcal{F}^2 = \int \varepsilon \cdot A^2 d\Omega \quad (9)$$

where  $\Omega$  is the solid angle, and integration of Eq. (9) is carried out over the angular domain of the polarimeter, efficiency  $\varepsilon = N_{ev}/N_{inc}$ , where  $N_{ev}$  is the number of useful events detected and  $N_{inc}$  is the number of incident particles,  $A$  is the analyzing power.

In our case the number of incident particles  $N_{inc}$  has been evaluated from the number of p–p quasi-elastic events at  $90^\circ$  in c.m. detected within the solid angle of  $7.56 \times 10^{-3}$  sr. The estimation of figures of merit was done as a sum over all the scintillation counters for d–p elastic events detection for the scattering angles of  $75^\circ$ – $135^\circ$  in c.m. Figures of merit  $\mathcal{F}_y$ ,  $\mathcal{F}_{yy}$  and  $\mathcal{F}_{xx}$  were estimated as  $\sim 1.6 \times 10^{-4}$ ,  $\sim 2.1 \times 10^{-4}$  and  $\sim 0.6 \times 10^{-4}$ , respectively.

These values are comparable with the figures of merit for the deuteron polarimeter used at the extracted beam at RIKEN [4]. However, in contrast with the RIKEN polarimeter [4] the large values of figures of merit were obtained with a very thin  $\text{CH}_2$  target  $10 \mu\text{m}$  thick using the internal beam. Estimated from p–p quasi-elastic scattering at  $90^\circ$  in c.m. the averaged luminosity was  $\mathcal{L} \sim 5.2 \times 10^{28} \text{ cm}^{-2}$  per beam spill. This value corresponds to the

$\text{CH}_2$  target effective length of  $\sim 5.2 \times 10^{21} \text{ g/cm}^2$  (0.6 mm) for the external beam with the averaged intensity of  $10^7$  deuterons per spill.

The performance of the polarimeter can be increased by the extension of the detection system to smaller scattering angles in c.m., since in this region the cross-section of d–p elastic scattering is larger and the analyzing powers have non-zero values. The detection of d–p elastic scattering at small angles in c.m. is especially important at higher energies since the cross-section decreases significantly.

The current polarimeter can be used in a wide deuteron energy range. The current setup was used to measure analyzing powers in d–p elastic scattering at higher energies [30] to study three-nucleon correlations.

## 5. Conclusions

A new polarimeter based on d–p elastic scattering has been installed at the internal beam of the Nuclotron. Measurements of the deuteron beam polarization have been performed at 270 MeV using precise data on the d–p elastic scattering analyzing powers obtained previously at RIKEN [1–4].

The detection at several scattering angles was used to compensate the low intensity of the polarized beam from POLARIS [27].

The figures of merit achieved are comparable with the ones for the external beam polarimeter at RIKEN [4] since the internal beam of the Nuclotron performs multi passages through the thin  $\text{CH}_2$  target.

The systematic error due to the uncertainties in the values of the analyzing powers does not exceed 1–2% for both the vector and tensor beam polarizations.

The measurements performed at 880 and 2000 MeV using the current setup have shown large values of the vector and tensor analyzing powers [30]. Therefore, after calibration this polarimeter can be used in a wide deuteron energy range. The future upgrade of the polarized ion source at the LHEP-JINR Accelerator Complex [32] will greatly enhance the capability of the current setup to measure spin-observables of d–p scattering and allow to perform the polarimeter calibrations in a wide energy range. The beam polarization will be measured with the same setup at 270 MeV before and after the measurements at higher energies.

## Acknowledgments

The authors are grateful to the Nuclotron accelerator and POLARIS groups. They thank L.S. Azhgirey, Yu.S. Anisimov, E. Ayush, A.F. Elishev, V.I. Ivanov, L.V. Karnjushina, Z.P. Kuznezova, A.P. Laricheva, A.G. Litvinenko, V.G. Perevozchikov, V.M. Slepnev, Yu.V. Zanevsky and V.N. Zhmyrov for their help during the preparation and performance of the experiment. The investigation has been partly supported by the Grant-in-Aid for Scientific Research (Grant No. 14740151) of the Ministry of Education, Culture, Sports, Science, and Technology of Japan; by the Russian Foundation for Fundamental Research (Grants No. 07-02-00102-a and 10-02-00087-a); by the Grant Agency for Science at the Ministry of Education of the Slovak Republic (Grant No. 1/4010/07) and by a Special program of the Ministry of Education and Science of the Russian Federation (Grant RNP2.1.1.2512).

## References

- [1] N. Sakamoto, et al., Phys. Lett. B 367 (1996) 60.
- [2] K. Sekiguchi, et al., Phys. Rev. C 65 (2002) 034003.
- [3] K. Sekiguchi, et al., Phys. Rev. C 70 (2004) 014001.

- [4] K. Suda, et al., Nucl. Instr. and Meth. A 572 (2007) 745.
- [5] K. Sekiguchi, et al., Phys. Rev. C 79 (2009) 054008.
- [6] H. Mardanpour, et al., Eur. Phys. J. A 31 (2007) 383.
- [7] T. Yagita, et al., Mod. Phys. Lett. A 18 (2003) 322.
- [8] A.A. Mehmandoost-Khaje-Dad, et al., Phys. Lett. B 617 (2005) 18.
- [9] M. Eslami-Kalantari, et al., Mod. Phys. Lett. A 24 (2009) 839.
- [10] H.R. Amir-Ahmadi, et al., Phys. Rev. C 75 (2007) 041001 (R).
- [11] E. Stephan, et al., Phys. Rev. C 76 (2007) 057001.
- [12] A. Ramazani-Moghaddam-Arani, et al., Phys. Rev. C 78 (2008) 014006.
- [13] E. Stephan, et al., Phys. Rev. C 82 (2010) 014003.
- [14] R.V. Cadman, et al., Phys. Rev. Lett. 86 (2001) 967;  
B.v. Przewoski, et al., Phys. Rev. C 74 (2006) 064003.
- [15] T. Uesaka, et al., Phys. Part. Nucl. Lett. 3 (2006) 305.
- [16] K. Sekiguchi, et al., in: EPJ Web of Conferences, vol. 3, 2010, pp.05024.
- [17] V.G. Ableev, et al., Nucl. Instr. and Meth. A 306 (1991) 73.
- [18] M. Haji-Saied, et al., Phys. Rev. C 36 (1987) 2010.
- [19] V. Ghazikhanian, et al., Phys. Rev. C 43 (1987) 1532.
- [20] D. Chiladze, et al., Phys. Rev. ST Accel. Beams 9 (2006) 050101.
- [21] J. Arvieux, et al., Nucl. Phys. A 431 (1984) 613.
- [22] M. Garçon, et al., Nucl. Phys. A 458 (1986) 287.
- [23] R. Bieber, et al., Nucl. Instr. and Meth. A 457 (2001) 12.
- [24] M. Altmeier, et al., Eur. Phys. J. A 23 (2005) 351.
- [25] A.I. Malakhov, et al., Nucl. Instr. and Meth. A 440 (2000) 320;  
Yu.S. Anisimov, et al., in: Proceedings of the 7-th International Workshop on Relativistic Nuclear Physics, 25–30 August 2003, Stara Lesna, Slovak Republic, 2003, p.117.
- [26] H. Okamura, Nucl. Instr. and Meth. A 443 (2000) 194.
- [27] N.G. Anishchenko, et al., AIP Conf. Proc. 95 (1983) 445.
- [28] Yu.V. Gurchin, et al., Phys. Part. Nucl. Lett. 4 (2007) 263.
- [29] G.G. Ohlsen, Rep. Prog. Phys. 35 (1972) 717.
- [30] K. Suda, et al., AIP Conf. Proc. 915 (2007) 920;  
P.K. Kurilkin, et al., Eur. Phys. J. ST 162 (2008) 137.
- [31] L.S. Azhgirey, et al., Nucl. Instr. and Meth. A 497 (2003) 340.
- [32] V.V. Fimushkin, et al., Eur. Phys. J. ST 162 (2008) 275.